Imprinting of different types of graphene oxide with metal cations

IMPRINTING OF DIFFERENT TYPES OF GRAPHENE OXIDE WITH METAL CATIONS

Authors: Piotr Zabierowski[a,b], Josef Osička[c], Josef Šťastný[a], Jaroslav Filip[a*]

[a] Department of Environmental Protection Engineering, Tomas Bata University in Zlin, Faculty of Technology, Nad Ovcirnou 3685, Zlin 760 01, Czechia

[b] CNR – Istituto per i Processi Chimico-Fisici, Sezione di Bari, via E. Orabona, 4, 70126, Bari, Italy

[c] Centre of Polymer Systems, Tomas Bata University in Zlin, Trida Tomase Bati 5678, Zlin 760 01, Czechia

* corresponding author: J. Filip, e-mail jfilip@utb.cz

Keywords: graphene oxide, metal cations, electrochemical determination, toxic metals, ion imprinting

ABSTRACT

It is known that graphene oxide (GO) particles bear negatively charged oxygen moieties which can interact with cations, what has been several times employed in fabrication of electrochemical sensors for metals. In this work, for the first time GO was treated with Cu^{2+}, Cd^{2+} or Pb^{2+} cations in a way similar to the ion imprinting by simple incubation of the two components and the synthesized nanomaterials were then deposited on carbon electrode surface forming electrochemical sensors towards lead cations. It was found that simple filtration of GO is very efficient way for collection of GO particles that could be imprinted most efficiently in terms of high electrochemical response towards lead cations. Part of the success also lies in high redox potential of Cu^{2+} that turned to be the best choice for the GO imprinting. It was also proven that the electrodes modified with ion-imprinted GO could work as the sensors of Pb^{2+} in drop amount of solution as well as they provide stable response under flow-through cell conditions suitable, for example, for online monitoring of water quality.

1. INTRODUCTION

Heavy metal contamination of surface water [1,2], and most importantly the drinking water, states a serious problem both in developing countries, [3] facing starvation and shortage of potable water, [4] but also in already developed countries [5]. The interaction of running line water conditioners and disinfectants (such as chlorine, monochloramine) [6,7] with elements of hydraulic installations (not only made from metal but also from recycled plastics [8–10] might produce elevated levels of heavy metals. The regulation of heavy metallic elements speciation thus might pose difficulties, as a result of redox reactions involving light metals (such as aluminum, manganese and copper) [11] and the above-mentioned non-metals and organic conditioners. In very high doses lead affects both the cardiovascular and nervous systems and accumulates in the organs of the body [12]. Trace exposure to lead affects neuro-development of children, including intelligence quotient [5,13], thus the facile and real-time control of heavy metals levels in the running water is of importance especially for (waste)water treatment monitoring.

The most sensitive and accurate methods of determination of lead in environmental samples belong to the family of induced coupled plasma atomic absorption spectroscopy, reaching the limits of detection for the lead at the tenths of parts per billion (ppb) and attogram level [14]. However, in many cases, these methods require preconcentration steps or time-consuming preparation of samples making a real-time running water analysis with AAS rather cumbersome task. The more facile solution is deploying of electrochemical methods of determination of lead with a characteristic oxidation peak observed at around -0.7 V vs. SCE (at pH 7 in 0.1 M NaCl with carbon paste electrode) [15,16]. Especially, the stripping differential pulse voltammetry, square wave voltammetry and impedance spectroscopy offer fast, precise and low standard deviation results, applicable in the context of running water monitoring in real-time [17]. The limits of detection in the flow system water analysis with these methods rely on the deposition step, where the working electrode is polarized negatively at the potential of reduction of metal cations to be reduced, and

subsequently strip (oxidize), the deposited amount of metal.

Electrodes types used in the determination of lead with the discussed methods decide on not only sensitivity but also the availability of the method for everyday use. The mercury dropping electrodes used for many years with success [18,19] allow to achieve highly reproducible response within a wide linear dynamic range of concentrations, high resolution of neighboring peaks, vigorous hydrogen evolution and satisfactory signal-to-background characteristics. The reason for this performance comes from chemical nature of the metal itself (mercury forms amalgams with many heavy metals) and renewability of electrode surface. Regardless of their advantages, mercury electrodes have been gradually replaced due to the toxicity of mercury. Bismuth-based electrodes (bulk electrodes, carbon paste with bismuth oxide, thin-film Bi modified electrodes…) offer comparable sensitivity due to the efficient formation of liquid amalgams with heavy metals at the same time bismuth is classified as an environmentally friendly non-toxic metal [17,20]. With the deposition step, the limits of detection of such bismuth electrodes might over-perform the other techniques but the electrode preparation (especially in-situ electrodeposition of Bi film) does not always fit the demand of running water analysis in real-time.

Modification of electrodes with graphene oxide (GO) offer plenty of room for engineering of metal sensors, mainly due to the presence of oxygen moieties in GO structure [21,22] which function as cation bonding sites [23]. Such affinity towards GO was proved many times and turned very versatile especially in metal sequestration studies [24,25]. Furthermore, hydrophilic oxygen groups make GO water-soluble, facilitating its deposition on a plethora of substrates including paper, metal foil and recyclable ceramic substrates. It should be also noted that, when well-dispersed and exfoliated, individual nanosheets of GO are not rigid, they can be folded and crumpled based on the electrostatic properties of the GO surface [26]. From electrochemical point of view GO has lower electron conductivity compared to graphene, due to the oxidation-induced disruption of in-plane system of conjugated double bonds. Although the oxygen moieties may catalyze certain electrochemical reactions [27], other reactions may be hindered by it [28]. Such a

drawback can be overcome by diverse methods of GO reduction, including electrochemical, chemical or thermal [29]. For example, Ramesha and Sampath synthesized lead dioxide-reduced graphene oxide nanohybrid applicable in electrochemical sensing of arsenic [30]. Other examples of graphene oxide-derived materials employed for the same purpose can be found in a 2019 review by Zuo et al. [31]

Based on the above-mentioned facts, it seems very reasonable to modify electrodes by GO in order to increase their voltammetric response towards Pb^{2+} cations. Unlike in the studies where "simple" GO was employed as enhancer of surface coverage of metal cations [32], the assembly of GO can be tailored by factors such as presence of cations [26] to affect the pore structure prior its deposition on the electrode surface. This treatment gained the possibility to selectively attract aqua-ions of heavy metals upon negative deposition potentials and reduce them within the pores in process of their determination using stripping voltammetry. This work is the first report on the tailoring of GO properties by simple incubation in a solution of diverse metal cations which can be labelled to as ion-imprinting and, to the best of the authors' knowledge, it has not been employed for preparation of toxic metal sensors previously. It is also known that different routes of GO synthesis provide material with diverse properties [33–35] and it can be anticipated that ion-imprinting of various GO would lead to various materials. For the first time, in this paper three types of graphene oxide (Hummer's, Brodie's and commercially available GO) have been ion-imprinted with different metal cations and the effect of such treatment on voltammetric response towards Pb^{2+} was investigated.

2. MATERIALS AND METHODS

2.1 Chemicals

Sodium, copper and cadmium nitrates, lead acetate, were obtained from VWR International. Commercially available graphene oxide (GOS; 4 mg mL^{-1} aqueous dispersion) was purchased from Sigma-Aldrich. Other chemicals (nitric acid, sodium hydroxide…) were of analytical grade. All

chemicals were used as received. For solution preparation, deionized water (DW) was used. Graphene oxide prepared according to Brodie and according to Hummers (GOB and GOS, respectively) were synthesized as follows:

GOB – while cooled in water/ice bath, fuming nitric acid (125 mL) and graphite (10 g) were stirred to obtain homogeneous dispersion into which potassium chlorate was added (50 g), followed by stirring for 20 h at 40 °C. Final step was 3-times repeated cleaning comprising of dilution with DW and centrifugation

GOH – while cooled in water/ice bath, concentrated sulfuric acid (100 mL) and graphite (5 g) were stirred to obtain homogeneous dispersion into which potassium manganate and sodium nitrate were added (15 and 6.5 g, respectively), followed by stirring for 6 h, addition of concentrated hydrogen peroxide (40 mL) and DW (300 mL) and final separation of product using centrifugation and washing with DW.

Both synthesized GOB and GOH were further cleaned from metal impurities with chloric acid (5%), followed again by washing with DW and centrifugation and the final freeze-drying.

2.2 Preparation of sensors

Three types of sensors prepared based on different treatment of the used graphene oxide. They have been labelled as “series 1”, “series S” and “series F” to distinguish whether an untreated GO, acidified and sedimented GO or filtrated GO were used, respectively. All sensors were prepared by modification with the prepared GO dispersions of commercially available screen-printed carbon electrodes (SPE; ref. 110, DropSens, Spain) with working and counter electrode from carbon paste and silver reference electrode deposited on 33x10 mm ceramic solid substrate. Working electrode is 4 mm in diameter.

2.2.1 “series 1”

Graphene oxide prepared according to the Brodie´s method (GOB) was dispersed in distilled water with a help of ultrasonic bath to achieve a 4 mg mL^{-1} dispersion. Then, 51 μL of the GOB

dispersion was mixed with 649 μL of DW and 600 μL of either 10 ppm solution of Pb^{2+}, Cu^{2+} or Cd^{2+} (aqueous solutions of respective nitrates) or $NaNO_3$. The mixtures in Eppendorf tubes were kept for 30 min to incubate, after that time they were drop-casted on surface of working electrodes of SPEs. Such modified electrodes were treated at 110°C for 15 min. In this way, electrodes denoted to as GO1 and **GO1-m** ("m" standing for Pb, Cu or Cd to assign which metal cation was employed for ion imprint) were prepared with the foremost one being modified only with GOB while GO1-m were modified with Pb-, Cu- or Cd-imprinted GOB.

2.2.2 "series S"

Graphene oxide prepared according to the Brodie´s (GOB) or Hummers´ (GOH) method were dispersed in 0.01M HNO_3 with a help of ultrasonic bath to achieve 4 mg mL^{-1} dispersions. Then the solutions were allowed to sedimentation at room temperature for 30 min and 50 μL of the resulting supernatants were mixed with 1-8 μL of 0.001 M Cu^{2+}, Cd^{2+} and Pb^{2+} in 0.01 M HNO_3 and 1240 μL of DW. These mixtures were left to incubate at room temperature for 15 minutes and then casted in aliquots of 25 μL at the working surface of the DRP-C110 electrodes and aged at 100°C for 15 min. Prior to measurements the electrodes were several times rinsed with DW. In this way, electrodes denoted to as **GOx-S** and **GOx-S-m** were prepared with "x" standing for B, H or S to distinguish the Brodie´s, Hummers´ and commercially available GO, respectively and "m" standing for Pb, Cu or Cd to assign which metal cations were employed for ion imprinting.

2.2.3 "series F"

The as-received 4 mg mL^{-1} Sigma Aldrich GO was diluted with 0.01M HNO_3 and sonicated for 15 minutes in ultrasonic bath to achieve 1 mg mL^{-1} dispersion (GOS). 10mg mL^{-1} GOB and GOH dispersions in DW were prepared with a help of ultrasonic bath for 15 min. The achieved GOS, GOB and GOH dispersions were filtered over a small column (1-2 cm), filled densely with filter paper to result in ca. 3 mL clarified suspensions aliquots. The filtrates achieved from GOB and GOH were additionally diluted each with 5 mL of 0.01M HNO_3. To achieve GOx-F-m solutions, 50 μL of the achieved GOx-F dispersions were mixed with 1-8 μL of 0.001 M Cu^{2+}, Cd^{2+} and Pb^{2+} in

0.01 M HNO_3 and 1240 μL of 0.9mM HNO_3. These mixtures were left to incubate at room temperature for 15 minutes and then casted in aliquots of 15 microliters at the working surface of the SPE electrodes and dried at 100°C for 15 min. Prior to measurements the electrodes were several times rinsed with DW. In this way, electrodes denoted to as **GOx-F** and **GOx-F-m** were prepared with "x" standing for B, H or S to distinguish the Brodie´s, Hummers´ and commercially available GO, respectively and "m" standing for Pb, Cu or Cd to assign which metal cations were employed for ion imprinting.

2.3 Electrochemical measurements

Unless stated otherwise, anodic stripping square wave voltammetry (ASSWV) measurements were done in potentiostatic mode using AUTOLAB PGSTAT302N (Metrohm, The Netherlands) with deposition potential -1.0 V, deposition time 60 s, modulation amplitude 0.02 V and frequency 25 Hz. The experimental data were collected and treated with NOVA 2.1 (Metrohm, The Netherlands) software. The modified SPE electrodes were placed in the flow cell with sub-mL volume (FLWCL; DropSens, Spain). The complete setup further contained a container with the electrolyte and peristaltic pump (2PP.M10; BVT Technologies, Czechia) connected with tubing to achieve the closed circulation system. For certain measurements, the modified SPEs were placed into designated SPE holder (DropSens), 50 μL drop of the analyzed solution was pipetted on their surface such as to cover all three electrodes and the measurement (ASSWV) was run under free atmosphere, room temperature.

2.4 Spectroscopic methods

The UV-vis spectra of analyzed dispersions placed into quartz cuvettes (optical path 10 mm) were recorded on Unicam UV 500 spectrometer (TE Instruments, USA) in the range from 200 to 850 nm with the use of deuterium lamp as a light source.

The FTIR spectra were recorded at Nicollette IQ10 spectrometer (Thermo Scientific, USA). The samples were prepared by casting the requested dispersions on pre-cleaned alumina foil,

following either drying in a nitrogen stream, room temperature, or thermal treatment equal to the one applied for preparation of the electrodes. All spectra were treated by Auto Smooth and Auto Baseline correction functions of Omnic software (Thermo Scientific, USA) before the peak height and position evaluation.

3. RESULTS

3.1 GO1-m sensors

As the first step in the study, the best conditions were sought for modification of SPE electrodes with GO-derived dispersions. For this purpose, GO1 and GO1-m sensors were prepared with thermal treatment of the modified SPEs at the temperature range from 80 to 400 °C. Following ASSWV measurements (100 mM KCl, pH 2.2 + 1 ppm Pb^{2+} circulating through the flow cell in a rate of 1.8 mL min^{-1}) revealed that, except for the electrodes treated at 300 and 400°C, anodic SWV peak attributed to the oxidation of deposited Pb^0 was always present and the highest peak was found at electrode prepared by drying at 100°C (7.8±1.3 μA, compared to 2.1±1.5 and 5.3±2.1 μA achieved with GO1-Pb sensors treated at 80 and 200 °C, respectively). Respective voltammograms are shown in **Fig. S1**, where it is also shown that no peaks could be observed when the sensors were treated at 300 and 400 °C. It underlines the necessity of oxygen moieties to capture metal cations and confirms that the high electron conductivity is not enough for ASSWV performance with metal cations. That the oxygen moieties were retained after 100°C thermal treatment was confirmed also by FTIR. Five main absorption band emerged, namely at about 1600, 1378, 1051, 945 and 827 cm^{-1} (**Fig. S2**). They can be assigned to sp2-hybridized carbon, hydroxyl (either from carboxyls, adsorbed water, or in a phenolic form) and epoxidic groups of graphene oxide [36]. Furthermore, the observed low level of reduction is consistent with literature. For example, Sheng at al. [37] confirmed that the thermal treatment of GO at 150°C retains oxygen groups while it increased the conductivity slightly above the initial GO´s value [37] and Shen et al. reported very mild level of reduction of GO at 100°C and shorter time (e.g. 1 h) [38]. It was also found that integration of Pb^{2+}

with GOB could not change the position of the observed absorption band significantly (**Fig. S2**) suggesting that the level of electrostatic interactions between the two components was surprisingly low.

For more detailed FTIR analysis, dispersions of GO1-Pb were prepared using the same procedure as described in the section 2.2.1, with various Pb^{2+} concentrations in the incubation solution. Moreover, GO1-Pb dispersions where GOH was employed instead of GOB were prepared. All dispersions were deposited on Al foil and treated at 100°C in order to achieve samples for FTIR analysis, as described in the section 2.4. Absorption intensities read from the acquired FTIR spectra were plotted towards the concentration of Pb^{2+} in the incubation solution as shown in the **Fig. S2**. The analysis revealed that for both types of GO1-Pb relative intensities at wavenumbers higher than 936 cm^{-1} decreased after integration of GOB or GOH with Pb^{2+}. This effect seems to be independent to the Pb^{2+} concentration at GO1-Pb samples prepared from GOH (**Fig. S3 a)** and **c)**) while certain dependence is observed for the GO1-Pb prepared with GOB (**Fig. S3 b)** and **d)**). It should be also noted that the latter set of samples exhibit the opposite trend when highest Pb^{2+} concentration is applied, that is, relative absorption intensity returns to the value of untreated GOB. Overall, the observed absorption decrease should be assigned to the acidic protons in Pb^{2+} solution rather than any strong interaction of Pb^{2+} ions with GOH or GOB. The partial dependence of absorption on Pb^{2+} concentration at GOB-containing samples suggests that GOB contains less pH-dependent oxygen moieties, which is in agreement with literature [39]. It should be also noted that the described different patterns of absorbance changes induced by Pb^{2+} solution addition can be observed very well at low wavelength region (Fig. S3 **a)** and **c)**), however assigning these bands to specific moieties may bring high level of uncertainty. Generally, epoxide groups can display as the absorption at about 800-900 cm^{-1} [36].

The prepared sensors were additionally compared with sensors prepared using solvothermal method which is known to be a mild reducing method for GO (employing either non-aqueous [40] or aqueous [41] dispersion). Here, GO1-Pb mixture in a glass capped bottle was placed into Teflon-

lined autoclave to undergo 15 min 120°C treatment. The treated dispersion was pipetted on SPE electrodes and dried under the nitrogen stream, room temperature, before placing into the flow cell. These hydrothermally treated GO1-Pb exhibited lower peak heights compared to thermally treated electrodes (ASSWV peak height of 6.9±3 and 12.0±3.8 μA for the former and the latter, respectively; data not shown). It may be related to further disruption of the conductive system of GO. Hence, for further experiments 15 min 100°C treatment in laboratory oven was chosen as the optimal modification protocol.

Under the conditions described above, the GO1 sensor have exhibited the stabilized response of 16.0±0.7 μA while GO1-Pb provided average response of 15.1±1.3 μA. Therefore, in a following series of experiments, pH of Pb^{2+} solution used for preparation of GO1-m was decreased using HNO_3 from close to neutral to value of 2. The acidic environment is known to improve solubility of most metals as a result of higher level of ionization, therefore the sorption to graphene oxide´s oxygen moieties may be more efficient. On the other side, pKa of graphene oxide´s carboxyls is about 4.5 [42] suggesting that the higher the pH the higher the GO´s negative charge responsible for higher capacity to bind divalent metal cations, as suggested for example by Tang et al. [43]. Regardless of this, the ASSWV peak heights achieved with acidified sensors (**Fig. 1**) were 16.7, 44.0 and 33.1% higher (for GO1-Pb, GO1-Cu and GO1-Cd, respectively) compared to GO1 sensor. Interestingly, Cu cations were the ones that increased the voltammetric response the most, compared to Pb and Cd. Regarding this, it should be considered GO1-m sensors were fabricated with the same weight concentration of metal cations, which is equal the molar ratio of Pb:Cd:Cu is 1:1.84:3.25 (based on different molar mass of the Pb^{2+}, Cd^{2+} and Cu^{2+}. In further experiments, equimolar concentrations were employed to be sure that the observed effect of Cu^{2+} is not stemming from simple “outnumbering” the other cations. It should be also noted that the calculated weight ratio of metal cations to the mass of GO in GO1-m is 29.4 mg of m^{2+} per 1 g of GO. Nováček et al. [44] have reported sorption capacity (not restricted by low concentration of metal in the solution) between 3.2 and 19.2 mg of Cd^{2+} per 1 g of GO (in “basic” state, without additional oxidation

which could improve the capacity), depending on GO preparation method [44]. It can be assumed that GO1-m were prepared in excess of metal cations.

This series of experiments revealed that 100°C treatment can be used for preparation of GOx-m sensors and that it is reasonable to acidify both the initial GOx-m dispersion as well as the supporting electrolyte during ASSWV.

Here Figure 1

3.2 GOx-S-m sensors

The first experiments of this series were focused on simple comparison of different types of GOx mixed with Pb in a concentration of 5.55 μM per 1 g of GOx (that is, 25-, 47- and 84-fold lower molar concentration of Pb^{2+}, Cd^{2+} and Cu^{2+}, respectively, compared to GO1-m sensors). Illustrative square wave voltammograms of GOx-S-Pb-modified and unmodified SPE electrodes are shown in the **Fig. 2 a)** which reveals that while employment of GOB-S-Pb and GOH-S-Pb increased the SWV peak heights by 35.9 and 57.9 %, respectively, employment of GOS under the same conditions decreased the voltammetric response by 35.3 %. Shapes of the voltammograms (**Fig. 2 a**) further revealed that the GOS-S-m resembles the unmodified electrode, concluding that GOS may not cover the working electrode active area as densely as GOB-S-Pb and GOH-S-Pb did. This study was further extended to examination of Cu^{2+} and Cd^{2+} in the same manner as Pb^{2+} with results shown in the **Fig. 2 b**. and respective voltammograms in **Fig. S4** (note that GOS-S-m sensors provided not very reliable response, therefore they were not included in the **Fig. S4**). Their integration has not caused as high peak increase as Pb^{2+} has. That leads to conclusion that Pb^{2+} can interact with GOH-S and GOB-S in a way resembling ion-imprinting, that is, certain structures are formed that can extract Pb^{2+} from solution more efficiently compared to structures formed by integration with Cd^{2+} and Cu^{2+}.

To further extend the study, GOx-S-m prepared with higher amounts of metal cations in the precursor solutions were investigated and the results are shown in the **Fig. S5**. None of these

sensors could provide a higher response compared to GOB-S-Pb and GOH-S-Pb prepared with 5.55 μM g^{-1} of Pb, showing possible ion-imprinting effect at non-saturated (in the mean of absorption capacity of GO) conditions. Regardless of a substantial ASSWV peak height increase after using 21.2 instead of 10.7 μM g^{-1} of Cd^{2+} and Cu^{2+} with GOH-S, the higher concentrations (up to 58.6 μM g^{-1}) have not exhibited any significant improvement in the response. The only exception is Cu^{2+} in combination with GOB-S (**Fig. S5 a**) which shown steady improvement of the recorded response upon increase of the amount of Cu^{2+} incubated with GOB-S.

Here Figure 2

From **Fig. 2** it is obvious that there are two components of the ASSWV peak assigned to the oxidation of Pb^0 deposited in the deposition step on electrode surface. It was suggested by Prof. Compton´s group [45] (Tibbetts, Davis and Compton, 2000) and later observed by others (for example [46–48]) that during ASSWV method intermetallic compounds can be formed that are oxidized at different (higher) potential than the pristine metal. From **Fig. 2** and **S5** it can be inferred that the observed effect is not a result of intermetallic compound formed from Pb^{2+} in the electrolyte and the metal cations imprinted into GOx-S deposited on the electrode. This assumption is based on facts that i) very significant peak separation could be observed also when pristine SPE (without addition of imprinting metal) was investigated and ii) peak positions are very similar, regardless of type of the imprinting metal (see **Fig. S5**; GOS-S-m sensors provided not very reliable response under the tested conditions, therefore they were not included in the **Fig. S5**.). Hence, the probable explanation was that acidic electrolyte caused partial desorption of silver from the reference electrode of SPE, which interacted with lead cations. This is supported by the presence of anodic peak at about 0 V which is potential close to oxidation of silver chloride, as described elsewhere [49–51] (note that Cl^- ions are present in the electrolyte in huge excess). Such behavior may be strengthened by dynamic conditions during the measurements (electrolyte circulation). More details about this issue are discussed in the section 4.2.

Taking the above-mentioned reasoning into account, it seems worthy to investigate stability of the prepared sensors in terms of repeated ASSWV measurements. Results can be found in the **Fig. 3** where the achieved peak heights are plotted against the number of the consecutive ASSWV scan.

It was found that the relative standard deviation for Pb peak heights were 3.4 and 1.7%, respectively, for GOB-S-Pb and GOH-S-Pb for three consecutive scans. After that, electrodes were removed and washed with DW which caused steady increase in "AgCl" peak in case of GOB-S-Pb while the Pb peak height stabilized at 21.5% higher value than before washing, with an average peak height of 38.8 μA and individual values showing relative deviation of 4.2%. For GOH-S-Pb, the Pb peak dropped by 32% after the washing and its relative standard deviation worsen from 1.7 to 3.7%. It points to a good stability of the Pb peak while the AgCl peak height was prone to substantial changes in case of GOB-S-Pb. It can be concluded that GOH-S-Pb sensors are more stable. Furthermore, in the **Fig. S6** ASSWV peak acquired from consecutive voltammograms achieved with GOB-S-Cu and GOB-S-Cd sensors are shown. It was shown that the removing and rinsing of the electrodes caused temporal decrease of the Pb peak height, which was partially restored and stabilized after two repeated ASSWV scans. In both cases, it could not reach higher values as was observed in case of GOB-S-Pb. The AgCl peak height followed the same pattern when GOB-S-Cd was investigated (that is, steadily increase), but GOB-S-Cu shown more or less stable response after 5 ASSWV scans. It suggests that Cu is responsible for certain structural changes that prevent from oxidation of higher amount of AgCl, or it may prevent its formation during the ASSWV deposition.

Here Figure 3

In a context of repeated measurements, electrochemical reduction of GO caused during the application of negative deposition potential can be discussed. Stability of the Pb ASSWV peaks suggest that it may occur during only first few measurements in case of GOB-S-Cu and GOB-S-Cd.

These sensors exhibit increase of the peak height during first 3 scans, while GOB-S-Pb is stable from its beginning. These results suggest that any possible occurring electrochemical reduction does not significantly affect the Pb oxidation peak current. The same is valid for the second observed effect, that is, deposition of AgCl and its oxidation. Similarly, the stability of Pb peak height was recorded also for all GOH-S-Cu and GOH-S-Cd sensors (**Fig. S6 b**).

3.3 GOx-F-m sensors

To exclude possible negative effect of larger aggregates of GO, filtrated dispersions were employed prepared as described in the section 2.1.3. The ASSWV response of these sensors have been investigated in the same way as in the case of GOx-S-m sensors. The only difference was that the scanning potential range was narrowed to avoid the above-mentioned formation of the "AgCl" oxidation peak. It can be anticipated that the GOx-F particles remained in the solution will be predominantly small and with large surface potential. UV-vis determination of the respective dispersions (**Fig. 4**) indeed revealed absorption peak between 280 and 320 nm, attributed to C=O bonds [52]. On the other side, absorption at about 230 nm, which can be associated with C=C bonds in carbonic "backbone" of graphene [52] is not so much stronger than the one assigned to C=O. This is valid only for GOB-F and GOH-F where the filtration helped to remove large non-oxidized graphenic or graphitic particles. Strong absorption at 230 nm exhibited by GOS-F sample indicated presence of less oxidized particles which affected the electrochemical response discussed in the following paragraphs.

First, number of repeated ASSWV measurements were performed with "non-imprinted" GOS-F, GOH-F and GOB-F sensors. As shown in the **Fig. S7**, even after avoiding higher potentials during ASSWV, the resulting Pb oxidation peak still contained two overlapping anodic processes. It can be assumed that either the influence of other ion(s) present in the electrolyte (most probably Ag^+ from the reference electrode). The other possibility which considered different functionalities of GO bonding Pb^{2+} cations resulting in different complexes displaying finally as two individual

ASSWV peaks have been rejected regarding the fact that the same overlapping of two peaks was observed also on unmodified SPEs (see **Fig. S7 d**). Other feature of GOx-F sensors was their lower response towards 1 ppm Pb^{2+} compared to pristine SPE. While 14.2, 14.9 and 13.7 μA peak was observed for GOS-F, GOH-F and GOB-F, respectively, the sole, unmodified SPE shown 28.1 μA. Stability of GOx-F sensors was also checked by consequent ASSWV measurements (voltammograms in the **Fig. S7**) with results revealing an increase of ASSWV peak height, in 1 ppm Pb^{2+} by 4.5, 13.9 and 14.4 % for GOS-F, GOH-F and GOB-F, respectively, after 3 ASSWV scans. The former two sensors were tested further, showing the final increase by 7.1 and 17.4%, all expressed relative to the first ASSWV scan, after total of 6 scans. Such behavior suggest that partial electrochemical reduction may occur with every stripping voltammetry scan (namely at its deposition step), since the response of pristine SPE remained within 3.9 % relative standard deviation. What is also noteworthy is low level of signal change at GOS-F, which can be ascribed to the fact that this sample was acidified before the filtration step and not after it like the GOB and GOH samples (see the Materials and methods section).

Next, investigation of ion-imprinted GOx-F-m sensors was performed and the results in form of absolute peak heights are summarized in the **Fig. 5.** It can be assumed that in all cases the integration of metal cations into graphene oxide improved the ASSWV response towards 1 ppm Pb^{2+} with the relative increase summarized in the **table 1**. Herein, values are listed for the sensors fabricated from the GOx-F-m dispersion with three different concentrations of imprinting metal cations. It should be considered that these values are only approximate since the real concentrations of GOx dispersions after the filtration step are lower than the initial 4 mg mL^{-1} used for calculations.

Here Fig. 4 and Fig. 5

Table 1: increase (in %) of ASSWV peak for 1 ppm Pb^{2+} achieved with GOx-F-m sensors, relative to the response of the respective GOx-F sensors. Metal cation type "m" is indicated in the first line of the table, second line indicates GOx type. First ASSWV scans were employed for the evaluation.

relative m^{2+} concentration (μM per g of GOx-F)	m = Cu			m = Cd			m = Pb		
	GOH-F	GOB-F	GOS-F	GOH-F	GOB-F	GOS-F	GOH-F	GOB-F	GOS-F
10.7	51.1	98.2	62.7	42.3	26.0	15.0	42.0	30.2	15.1
21.2	71.8	83.7	75.8	28.8	47.5	20.0	15.6	18.9	23.1
26.6	80.4	72.2	29.6	36.5	50.2	7.3	30.1	25.4	-14.4

Unlike in the case of GOx-S-m sensors, GOx-F-m shown the best results when Cu^{2+} cations were used for imprinting. This was valid for all types of graphene oxide with GOB-F-Cu (at lowest Cu^{2+} concentration) showing the highest increase (by 98.2%) of the voltammetric peak for 1 ppm Pb^{2+} compared to GOB-F sensor. For comparison, imprinting of GOB-F with Cd^{2+} and Pb^{2+} lead only to the peak height increase by 26.0 and 30.2 %. The absolute peak height for the GOB-F-Cu was even comparable to unmodified SPE electrode and after three consecutive ASSWV scans it even surpassed it (see **Fig. 4 c**). It should be noted that the absolute amount of the imprinted graphene oxide on the electrode surface is lower compared to all previous experiments since some part of GO particles was removed by filtration. It is quite reasonable to presume that upon deposition of higher GOX-F-m amount on the electrode surface even higher response will be achieved although the confirmation of this hypothesis is not under the scope of this work. On the other side, such performance gain achieved with the reportedly low amount of the modification agent applied on the electrode is remarkable. Undoubtedly, the filtration step allowing for separation of the finest GO particles is crucial for further development of this type of electrochemical sensors.

4. DISCUSSION

The achieved results described above have suggested that the integration of metal cations during thermal treatment of graphene oxide increased the voltammetric response of the sensors towards lead cations. Hence, in this section two issues should be further discussed: 1) nature of integration of GO and metal cations; 2) sensing properties of the fabricated electrodes.

4.1 Integration of GO and metal cations

This problem can be divided into partial questions, including i) physical features (crumpling of GO sheets) and ii) the chemical ones.

i) In regard of structure of imprinted GO particles, it should be first noted that the partial negative charge of the GO´s oxygen moieties keeps the particles separated; once this charge is neutralized, aggregation of GO can be observed. The neutralization can be induced by a protonation occurring bellow GO´s estimated pKa, which is between pH of 4-4.5 [42,53]. Besides that, folding of GO at low pH can be fostered by forming of hydrogen bonds [25]. Importantly, the pH below pKa does not mean the complete absence of surface charge of GO at pH=2. For example, Orth et al. shown FTIR results of GO taken at pH 3 suggesting certain portion of carboxylic groups is left ionized [53], Konkena and Vasudevan reported zeta potential of GO at pH=2 to be about -15 mV [42] and Tang et al. have reported number of deprotonated groups on GO to be 0.41 mmol L^{-1} at pH=2 [43]. As a result, certain rate of metal cation binding will occur also under low pH conditions employed in our work.

Another option is compensation of the charge by counter-ions, including metal cations [54]. This is especially true for divalent (trivalent, tetravalent…) cations, while for instance monovalent Ag^{+} ions have not exhibited this effect [51]. Incebay and Yazicigil [26] have shown crumpling of graphene oxide deposited on GCE surface upon incubation of the electrode in the Cu^{2+} solution. From their text, however, it is not clear how fast the process is. On the other side, the coagulation of graphene oxide under the strong acidic conditions observed by naked eye is almost instant process (data not shown) hence it can be presumed that imprinting of metal cation under herein studied conditions is also fast. Furthermore, from Incebay and Yazicigil results it is obvious that strong reduction of GO caused almost complete loss of capability to bind copper cations to the surface [26]. It is in agreement with our results, where high temperature treatment (> 300°C) of GO-modified SPE proven incapable of Pb sensing. An important aspect of GO modified by divalent

cations (Mg^{2+}, Ca^{2+}) was reported by Park et al. who pointed out that divalent ions could improve stability of graphene oxide papers via electrostatic crosslinking [55].

ii) It should be discussed why GOH-F-Cu combination provided the best results towards Pb sensing. First, graphene oxide flakes change their electrostatic binding properties upon separation of particles with different relative surface charge (respective to the estimated area of the particles, or nanosheets), as proven before [56]. The part of the success here is therefore the filtration step which helped to reject particles with improper cation-binding properties.

Second issue to consider is reductive potential of Cu^{2+}, Pb^{2+} and Cd^{2+} which are +0.34, -0.13 and -0.4 V vs. standard hydrogen electrode (SHE), respectively. On the other side, formal oxidative potential of GO is +0.724 vs. SHE [57]. It was shown that such difference in formal redox potential levels cause spontaneous reduction of metal cations in presence of GO, which is in turn oxidized [57–59]. It can be assumed that, compared to Cd^{2+} and Pb^{2+}, Cu^{2+} is the strongest oxidizing agent and will be the most prone to integrate with GO in their reduced form (i.e. metallic Cu agglomerates, particles). Hence, the "success" of Cu can be ascribed to the fact that it interact with GO in the most "active" way.

4.2 Electrochemical properties

Redha et al. shown differential pulse voltammograms for Pb^{2+} in glycine buffer, under the flow-cell conditions, with two peaks, although they do not make any comment on the phenomenon [60]. The same peak separation was observed by Sun et al., with their disk glassy carbon electrode coated by Fe_3O_4-decorated PVP-reduced graphene oxide nanohybrid [61]. This phenomenon, according to the literature [62,63], can be assigned to underpotential deposition (UPD) when metal cations are deposited at lower overpotential on a surface comprising of another material compared to deposition on surface formed of the same metal atoms [64]. What is intriguing is that, unlike the other authors describe, GOx-F-m sensors exhibit almost equally height peak for both UPD and bulk deposition. It is most probably connected to the leached silver described above and enhanced

distribution of both Pb^{2+} and Ag^{+} cations in the vicinity of the electrode surface caused by flowing of the electrolyte. It is also significant that this phenomenon is partially suppressed by the graphene oxide nanomaterials on the electrode, as inferred from the fact that the ratio between "UPD" and "bulk" peak heights were 1.72 for SPE while it was, on average, 1.48 for GOx-F electrodes and with further measurement it stayed the same for SPE while it dropped down to 1.3 and even 1.2 during 2nd and 3rd ASSWV measurement, respectively, for GOx-F electrodes. In accordance with that, the "bulk" peaks surpassed in their height the "UPD" ones when GOx-S-m were used (see **Fig. S4**), which were prepared with non-filtered, more concentrated, GOx dispersions. This fact again supports the thesis that increasing of the GOx-F-m dispersions´ concentrations would be the way for significantly improve the sensing properties. However, these experiments are not within scope of the current work.

Although the intention of this work was to investigate the integration of graphene oxides with metal cations, a brief look at the sensing properties has been also taken to prove the concept. For this purpose, two GOH-F-Cd sensors, GOH-F-Cd1 and GOH-F-Cd2 prepared with 26.6 and 31.8 μM Cd^{2+} per g of GOH-F, respectively, were investigated. With these, ASSWV was taken with 1, 2 and 3 ppm of Pb^{2+} in 50 μL solution dropped directly on the sensor surface (**Fig. 6)**. The sensitivity of 38.2±4.5 (for GOH-F-Cd1) and 26.3±2.8 (for GOH-F-Cd2) μA ppm^{-1} and limit of detection of 177 and 218 ppb were achieved. Seenivasan et al. have reported maximum sensitivity of only 18.4 μA ppm^{-1} for their cysteine-modified graphene oxide at polypyrrole matrix nanohybrid on SPE electrode and 100 μL of sample dropped on the sensor surface [65]. It was lower than 31.8 μA ppm^{-1} achieved with simple reduced graphene oxide-modified SPE reported by Jian et al. [32] while Mandil et al. reported 210 μA ppm^{-1}, but their technique employed preconcentration step [66]. Zhan et al. reported 185 μA ppm^{-1} sensitivity, with SPE modified by zinc oxide nanoparticles and reduced graphene oxide in nafion matrix dipped in larger volume (compared to in-drop solution) of the sample [67]. It can be assumed that the prepared ion-imprinted graphene oxide sensors fit well into performance of graphene-modified SPE, measurement in a drop. Furthermore, this research has

opened the way for further development of online flow-through sensors proving that metal cations (especially Cu^{2+}) integrated with graphene oxide are very suitable coating nanomaterials for carbon electrodes.

Here Figure 6

5. CONCLUSIONS

In this work interaction of three types of graphene oxide with Pb^{2+}, Cd^{2+} and Cu^{2+} cations under different conditions was investigated. The resulted nanomaterials prepared by simple incubation of dispersions of graphene oxide and solutions of the respective cations, in a process resembling ion imprinting, were further tested as a coating material of SPE carbon electrodes to develop a fundament for online electrochemical detection of potentially toxic metals. The major findings are that exclusion of larger GO particles using simple filtration with filtration paper is a crucial step in using such metal cation imprinting of GO. Indeed, the ion-imprinting of filtrated GO particles displayed as a significant increase of a voltammetric response towards Pb^{2+} cations, compared with "blank" sensors fabricated with pristine filtrated GO. Another crucial point was presence of oxygen moieties on GO surface since no reliable signal was recorded after application of high temperature (>200°C) associated with reduction process. Therefore, 100°C treatment was found as the optimum between the requirement of fast drying and low level of reduction. The third major finding is that when ion-imprinting is performed with filtrated GO, chemical properties of Cu^{2+} (which is stronger oxidant than Cd^{2+} a Pb^{2+}) come into play leading to the imprinted GO most suitable for fabrication of metal sensors. This was not obvious when larger particles (with less "active" electron-donating moieties in bulk of GO) were ion-imprinted; in such case, Pb^{2+} could imprinted GO in the way most suitable for detection of Pb. Last but not least, linear dependence of the voltammetric peak height and Pb^{2+} concentration in the electrolyte was observed proving the applicability of the ion-imprinted GO in fabrication of electrochemical sensors towards potentially toxic metals in water.

Acknowledgements

This work was supported by Czech science foundation [grant number GAČR 20-27735Y].

REFERENCES

[1] M.I. Ahamed, E. Lichtfouse, Water pollution and remediation: Heavy metals, Springer, 2020.
[2] B. Sarkar, Heavy metals in the environment, CRC press, 2002.
[3] G.E. Zaikov, L.I. Weisfeld, E.M. Lisitsyn, S.A. Bekuzarova, Heavy metals and other pollutants in the environment: biological aspects, CRC Press, 2017.
[4] S.K. Sharma, Heavy metals in water : presence, removal and safety, Gld, Royal Society of Chemistry, 2014. http://gen.lib.rus.ec/book/index.php?md5=8ecadb210da3aac05a86947b62523e3f.
[5] P.S. Rawat, S. Singh, A.A. Mahdi, S. Mehrotra, Environmental Lead exposure and its Correlation with Intelligence Quotient level in Children, J. Trace Elem. Med. Biol. (2022) 126981. https://doi.org/10.1016/j.jtemb.2022.126981.
[6] J.A. Switzer, V. V Rajasekharan, S. Boonsalee, E.A. Kulp, E.W. Bohannan, Evidence that Monochloramine Disinfectant Could Lead to Elevated Pb Levels in Drinking Water, Environ. Sci. Technol. 40 (2006) 3384–3387. https://doi.org/10.1021/es052411r.
[7] V. V Rajasekharan, B.N. Clark, S. Boonsalee, J.A. Switzer, Electrochemistry of Free Chlorine and Monochloramine and its Relevance to the Presence of Pb in Drinking Water, Environ. Sci. Technol. 41 (2007) 4252–4257. https://doi.org/10.1021/es062922t.
[8] A. Turner, M. Filella, Lead in plastics - Recycling of legacy material and appropriateness of current regulations, J. Hazard. Mater. 404 (2021) 124131. https://doi.org/10.1016/j.jhazmat.2020.124131.
[9] A. Turner, Black plastics: Linear and circular economies, hazardous additives and marine pollution, Environ. Int. 117 (2018) 308–318. https://doi.org/10.1016/j.envint.2018.04.036.
[10] B.P. Lanphear, Low-level toxicity of chemicals: No acceptable levels?, {PLOS} Biol. 15 (2017) e2003066. https://doi.org/10.1371/journal.pbio.2003066.
[11] G. Li, Y. Bae, A. Mishrra, B. Shi, D.E. Giammar, Effect of Aluminum on Lead Release to Drinking Water from Scales of Corrosion Products, Environ. Sci. Technol. 54 (2020) 6142–6151. https://doi.org/10.1021/acs.est.0c00738.
[12] M. Faisal, Q. Saquib, A.A. Alatar, A.A. Al-Khedhairy, Cellular and Molecular Phytotoxicity of Heavy Metals, Springer, 2020.
[13] I.C. Dike, C.N. Onwurah, U. Uzodinma, I.N. Onwurah, Evaluation of Pb concentrations in selected vegetables and portable drinking water, and intelligent quotients of school children in Ishiagu - a Pb mining community: health risk assessment using predictive modelling, Environ. Monit. Assess. 192 (2020) 1–13. https://doi.org/10.1007/s10661-020-8071-2.
[14] K.V. Baskaran, G. Blanchet-Chouinard, D. Larivi\a`ere, Attogram measurement of ^{210}Pb in drinking water by ICP-MS/MS, J. Anal. At. Spectrom. 33 (2018) 603–612. https://doi.org/10.1039/c7ja00408g.
[15] C. Laghlimi, Y. Ziat, A. Moutcine, M. Hammi, Z. Zarhri, R. Maallah, O. Ifguis, A. Chtaini, Analysis of Pb(II), Cu(II) and Co(II) in drinking water by a new carbon paste electrode modified with an organic molecule, Chem. Data Collect. 29 (2020) 100496. https://doi.org/10.1016/j.cdc.2020.100496.
[16] R. Pauliukaite, R. Metelka, I. Švancara, A. Królicka, A. Bobrowski, K. Vytřas, E. Norkus, K. Kalcher, Carbon paste electrodes modified with Bi 2 O 3 as sensors for the determination of

Cd and Pb, Anal. Bioanal. Chem. 374 (2002) 1155–1158. https://doi.org/10.1007/s00216-002-1569-3.
[17] J. Wang, Stripping Analysis at Bismuth Electrodes: A Review, Electroanalysis. 17 (2005) 1341–1346. https://doi.org/10.1002/elan.200403270.
[18] V. Vyskočil, J. Barek, Mercury Electrodes–Possibilities and Limitations in Environmental Electroanalysis, Crit. Rev. Anal. Chem. 39 (2009) 173–188. https://doi.org/10.1080/10408340903011820.
[19] J.H. Christie, J.A. Turner, R.A. Osteryoung, Square wave voltammetry at the dropping mercury electrode: theory, Anal. Chem. 49 (1977) 1899–1903. https://doi.org/10.1021/ac50021a008.
[20] F. Arduini, J.Q. Calvo, G. Palleschi, D. Moscone, A. Amine, Bismuth-modified electrodes for lead detection, TrAC Trends Anal. Chem. 29 (2010) 1295–1304. https://doi.org/https://doi.org/10.1016/j.trac.2010.08.003.
[21] J.P. Rourke, P.A. Pandey, J.J. Moore, M. Bates, I.A. Kinloch, R.J. Young, N.R. Wilson, The Real Graphene Oxide Revealed: Stripping the Oxidative Debris from the Graphene-like Sheets, Angew. Chemie Int. Ed. 50 (2011) 3173–3177. https://doi.org/https://doi.org/10.1002/anie.201007520.
[22] D.R. Dreyer, S. Park, C.W. Bielawski, R.S. Ruoff, The chemistry of graphene oxide, Chem. Soc. Rev. 39 (2010) 228–240. https://doi.org/10.1039/B917103G.
[23] S.Z.N. Ahmad, W.N. Wan Salleh, A.F. Ismail, N. Yusof, M.Z. Mohd Yusop, F. Aziz, Adsorptive removal of heavy metal ions using graphene-based nanomaterials: Toxicity, roles of functional groups and mechanisms, Chemosphere. 248 (2020) 126008. https://doi.org/10.1016/j.chemosphere.2020.126008.
[24] N. Nirmala, V. Shriniti, K. Aasresha, J. Arun, K.P. Gopinath, S.S. Dawn, A. Sheeladevi, P. Priyadharsini, K. Birindhadevi, N.T.L. Chi, A. Pugazhendhi, Removal of toxic metals from wastewater environment by graphene-based composites: A review on isotherm and kinetic models, recent trends, challenges and future directions, Sci. Total Environ. 840 (2022) 156564. https://doi.org/10.1016/j.scitotenv.2022.156564.
[25] R. Sitko, E. Turek, B. Zawisza, E. Malicka, E. Talik, J. Heimann, A. Gagor, B. Feist, R. Wrzalik, Adsorption of divalent metal ions from aqueous solutions using graphene oxide, Dalt. Trans. 42 (2013) 5682–5689. https://doi.org/10.1039/C3DT33097D.
[26] H. İncebay, Z. Yazıcıgil, Effect of different copper salts on the electrochemical determination of Cu(II) by the application of the graphene oxide-modified glassy carbon electrode, Surfaces and Interfaces. 9 (2017) 160–166. https://doi.org/10.1016/j.surfin.2017.09.004.
[27] D.A.C. Brownson, A.C. Lacombe, M. Gómez-Mingot, C.E. Banks, Graphene oxide gives rise to unique and intriguing voltammetry, RSC Adv. 2 (2012) 665–668. https://doi.org/10.1039/C1RA00743B.
[28] J. Filip, J. Tkac, Effective bioelectrocatalysis of bilirubin oxidase on electrochemically reduced graphene oxide, Electrochem. Commun. 49 (2014) 70–74. https://doi.org/10.1016/j.elecom.2014.10.012.
[29] S. Pei, H.-M. Cheng, The reduction of graphene oxide, Carbon N. Y. 50 (2012) 3210–3228. https://doi.org/10.1016/j.carbon.2011.11.010.
[30] G.K. Ramesha, S. Sampath, In-situ formation of graphene–lead oxide composite and its use in trace arsenic detection, Sensors Actuators B Chem. 160 (2011) 306–311. https://doi.org/10.1016/j.snb.2011.07.053.
[31] Y. Zuo, J. Xu, X. Zhu, X. Duan, L. Lu, Y. Yu, Graphene-derived nanomaterials as recognition elements for electrochemical determination of heavy metal ions: a review, Microchim. Acta. 186 (2019) 171. https://doi.org/10.1007/s00604-019-3248-5.
[32] J.-M. Jian, Y.-Y. Liu, Y.-L. Zhang, X.-S. Guo, Q. Cai, Fast and Sensitive Detection of Pb2+ in Foods Using Disposable Screen-Printed Electrode Modified by Reduced Graphene Oxide, Sensors . 13 (2013). https://doi.org/10.3390/s131013063.
[33] J.G.S. Moo, B. Khezri, R.D. Webster, M. Pumera, Graphene Oxides Prepared by Hummers',

Hofmann's, and Staudenmaier's Methods: Dramatic Influences on Heavy-Metal-Ion Adsorption, ChemPhysChem. 15 (2014) 2922–2929. https://doi.org/10.1002/cphc.201402279.
[34] P. Feicht, J. Biskupek, T.E. Gorelik, J. Renner, C.E. Halbig, M. Maranska, F. Puchtler, U. Kaiser, S. Eigler, Brodie's or Hummers' Method: Oxidation Conditions Determine the Structure of Graphene Oxide, Chem. - A Eur. J. 25 (2019) 8955–8959. https://doi.org/10.1002/chem.201901499.
[35] W. Peng, H. Li, Y. Liu, S. Song, Comparison of Pb(II) adsorption onto graphene oxide prepared from natural graphites: Diagramming the Pb(II) adsorption sites, Appl. Surf. Sci. 364 (2016) 620–627. https://doi.org/10.1016/j.apsusc.2015.12.208.
[36] C. Zhang, D.M. Dabbs, L.-M. Liu, I.A. Aksay, R. Car, A. Selloni, Combined Effects of Functional Groups, Lattice Defects, and Edges in the Infrared Spectra of Graphene Oxide, J. Phys. Chem. C. 119 (2015) 18167–18176. https://doi.org/10.1021/acs.jpcc.5b02727.
[37] Y. Sheng, Y. Zhou, C. Tang, X. Cheng, C. Zhang, Redispersible Reduced Graphene Oxide Prepared in a Gradient Solvent System, Nanomater. 12 (2022). https://doi.org/10.3390/nano12121982.
[38] Y. Shen, S. Zhang, Y. Sun, C. Hai, X. Li, J. Zeng, X. Ren, Y. Zhou, Structure and Property Evolution of Graphene Oxide Sheets during Low-Temperature Reduction on a Solid Substrate, J. Phys. Chem. C. 124 (2020) 14371–14379. https://doi.org/10.1021/acs.jpcc.0c03499.
[39] S. You, S.M. Luzan, T. Szabó, A. V Talyzin, Effect of synthesis method on solvation and exfoliation of graphite oxide, Carbon N. Y. 52 (2013) 171–180. https://doi.org/10.1016/j.carbon.2012.09.018.
[40] H. Wang, J.T. Robinson, X. Li, H. Dai, Solvothermal Reduction of Chemically Exfoliated Graphene Sheets, J. Am. Chem. Soc. 131 (2009) 9910–9911. https://doi.org/10.1021/ja904251p.
[41] Z. Li, T. Huang, W. Gao, Z. Xu, D. Chang, C. Zhang, C. Gao, Hydrothermally Activated Graphene Fiber Fabrics for Textile Electrodes of Supercapacitors, ACS Nano. 11 (2017) 11056–11065. https://doi.org/10.1021/acsnano.7b05092.
[42] B. Konkena, S. Vasudevan, Understanding Aqueous Dispersibility of Graphene Oxide and Reduced Graphene Oxide through pKa Measurements, J. Phys. Chem. Lett. 3 (2012) 867–872. https://doi.org/10.1021/jz300236w.
[43] H. Tang, S. Zhang, T. Huang, J. Zhang, B. Xing, Mechanisms of the Aggregation of Graphene Oxide at High pH: Roles of Oxidation Debris and Metal Adsorption, Environ. Sci. Technol. 55 (2021) 14639–14648. https://doi.org/10.1021/acs.est.1c04463.
[44] M. Nováček, O. Jankovský, J. Luxa, D. Sedmidubský, M. Pumera, V. Fila, M. Lhotka, K. Klímová, S. Matějková, Z. Sofer, Tuning of graphene oxide composition by multiple oxidations for carbon dioxide storage and capture of toxic metals, J. Mater. Chem. A. 5 (2017) 2739–2748. https://doi.org/10.1039/C6TA03631G.
[45] D.F. Tibbetts, J. Davis, R.G. Compton, Sonoelectroanalytical detection of lead at a bare copper electrode, Fresenius. J. Anal. Chem. 368 (2000) 412–414. https://doi.org/10.1007/s002160000523.
[46] W. Xiong, L. Zhou, S. Liu, Development of gold-doped carbon foams as a sensitive electrochemical sensor for simultaneous determination of Pb (II) and Cu (II), Chem. Eng. J. 284 (2016) 650–656. https://doi.org/10.1016/j.cej.2015.09.013.
[47] Z. Zhong, A. Ali, R. Jamal, R. Simayi, L. Xiang, S. Ding, T. Abdiryim, Poly(EDOT-pyridine-EDOT) and poly(EDOT-pyridazine-EDOT) hollow nanosphere materials for the electrochemical detection of Pb^{2+} and Cu^{2+}, J. Electroanal. Chem. 822 (2018) 112–122. https://doi.org/10.1016/j.jelechem.2018.05.022.
[48] J. Sotolářová, Š. Vinter, J. Filip, Cellulose derivatives crosslinked by citric acid on electrode surface as a heavy metal absorption/sensing matrix, Colloids Surfaces A Physicochem. Eng. Asp. 628 (2021) 127242. https://doi.org/10.1016/j.colsurfa.2021.127242.

[49] J. Bujes-Garrido, D. Izquierdo-Bote, A. Heras, A. Colina, M.J. Arcos-Martínez, Determination of halides using Ag nanoparticles-modified disposable electrodes. A first approach to a wearable sensor for quantification of chloride ions, Anal. Chim. Acta. 1012 (2018) 42–48. https://doi.org/10.1016/j.aca.2018.01.063.
[50] M. Yu, P. Liu, S. Zhang, J. Liu, J. An, S. Li, Preparation of graphene–Ag composites and their application for electrochemical detection of chloride, Mater. Res. Bull. 47 (2012) 3206–3210. https://doi.org/10.1016/j.materresbull.2012.08.013.
[51] J. Filip, P. Wechsler, J. Stastny, V. Malkova, A. Minarik, S. Vinter, J. Osicka, Simplified synthesis of silver nanoparticles on graphene oxide and their applications in electrocatalysis, Nanotechnology. 32 (2020) 25502. https://doi.org/10.1088/1361-6528/abb8a4.
[52] R.D. Martínez-Orozco, H.C. Rosu, S.-W. Lee, V. Rodríguez-González, Understanding the adsorptive and photoactivity properties of Ag-graphene oxide nanocomposites, J. Hazard. Mater. 263 (2013) 52–60. https://doi.org/10.1016/j.jhazmat.2013.07.056.
[53] E.S. Orth, J.G.L. Ferreira, J.E.S. Fonsaca, S.F. Blaskievicz, S.H. Domingues, A. Dasgupta, M. Terrones, A.J.G. Zarbin, pKa determination of graphene-like materials: Validating chemical functionalization, J. Colloid Interface Sci. 467 (2016) 239–244. https://doi.org/10.1016/j.jcis.2016.01.013.
[54] Y. Gao, Y. Qin, M. Zhang, L. Xu, Z. Yang, Z. Xu, Y. Wang, M. Men, Revealing the role of oxygen-containing functional groups on graphene oxide for the highly efficient adsorption of thorium ions, J. Hazard. Mater. 436 (2022) 129148. https://doi.org/10.1016/j.jhazmat.2022.129148.
[55] S. Park, K.-S. Lee, G. Bozoklu, W. Cai, S.T. Nguyen, R.S. Ruoff, Graphene Oxide Papers Modified by Divalent Ions—Enhancing Mechanical Properties via Chemical Cross-Linking, ACS Nano. 2 (2008) 572–578. https://doi.org/10.1021/nn700349a.
[56] J. Filip, A. Andicsová-Eckstein, A. Vikartovská, J. Tkac, Immobilization of bilirubin oxidase on graphene oxide flakes with different negative charge density for oxygen reduction. The effect of GO charge density on enzyme coverage, electron transfer rate and current density, Biosens. Bioelectron. 89 (2017) 384–389. https://doi.org/10.1016/j.bios.2016.06.006.
[57] X. Chen, G. Wu, J. Chen, X. Chen, Z. Xie, X. Wang, Synthesis of "Clean" and Well-Dispersive Pd Nanoparticles with Excellent Electrocatalytic Property on Graphene Oxide, J. Am. Chem. Soc. 133 (2011) 3693–3695. https://doi.org/10.1021/ja110313d.
[58] K. Spilarewicz-Stanek, A. Kisielewska, J. Ginter, K. Bałuszyńska, I. Piwoński, Elucidation of the function of oxygen moieties on graphene oxide and reduced graphene oxide in the nucleation and growth of silver nanoparticles, RSC Adv. 6 (2016) 60056–60067. https://doi.org/10.1039/C6RA10483E.
[59] H.C. Choi, M. Shim, S. Bangsaruntip, H. Dai, Spontaneous Reduction of Metal Ions on the Sidewalls of Carbon Nanotubes, J. Am. Chem. Soc. 124 (2002) 9058–9059. https://doi.org/10.1021/ja026824t.
[60] Z.M. Redha, S.J. Baldock, P.R. Fielden, N.J. Goddard, B.J.T. Brown, B.G.D. Haggett, R. Andres, B.J. Birch, Hybrid Microfluidic Sensors Fabricated by Screen Printing and Injection Molding for Electrochemical and Electrochemiluminescence Detection, Electroanalysis. 21 (2009) 422–430. https://doi.org/10.1002/elan.200804415.
[61] Y. Sun, W. Zhang, H. Yu, C. Hou, D. Li, Y. Zhang, Y. Liu, Controlled synthesis various shapes Fe3O4 decorated reduced graphene oxide applied in the electrochemical detection, J. Alloys Compd. 638 (2015) 182–187. https://doi.org/10.1016/j.jallcom.2015.03.061.
[62] S. Muralikrishna, D.H. Nagaraju, R.G. Balakrishna, W. Surareungchai, T. Ramakrishnappa, A.B. Shivanandareddy, Hydrogels of polyaniline with graphene oxide for highly sensitive electrochemical determination of lead ions, Anal. Chim. Acta. 990 (2017) 67–77. https://doi.org/10.1016/j.aca.2017.09.008.
[63] Z. Wang, L. Li, E. Liu, Graphene ultrathin film electrodes modified with bismuth nanoparticles and polyaniline porous layers for detection of lead and cadmium ions in acetate buffer solutions, Thin Solid Films. 544 (2013) 362–367.

https://doi.org/10.1016/j.tsf.2013.02.098.
[64] E. Herrero, L.J. Buller, H.D. Abruña, Underpotential Deposition at Single Crystal Surfaces of Au, Pt, Ag and Other Materials, Chem. Rev. 101 (2001) 1897–1930. https://doi.org/10.1021/cr9600363.
[65] R. Seenivasan, W.-J. Chang, S. Gunasekaran, Highly Sensitive Detection and Removal of Lead Ions in Water Using Cysteine-Functionalized Graphene Oxide/Polypyrrole Nanocomposite Film Electrode, ACS Appl. Mater. Interfaces. 7 (2015) 15935–15943. https://doi.org/10.1021/acsami.5b03904.
[66] A. Mandil, L. Idrissi, A. Amine, Stripping voltammetric determination of mercury(II) and lead(II) using screen-printed electrodes modified with gold films, and metal ion preconcentration with thiol-modified magnetic particles, Microchim. Acta. 170 (2010) 299–305. https://doi.org/10.1007/s00604-010-0329-x.
[67] W. Zhang, Y. Xu, X. Zou, A ZnO–RGO-modified electrode coupled to microwave digestion for the determination of trace cadmium and lead in six species fish, Anal. Methods. 9 (2017) 4418–4424. https://doi.org/10.1039/C7AY01574G.

FIGURES

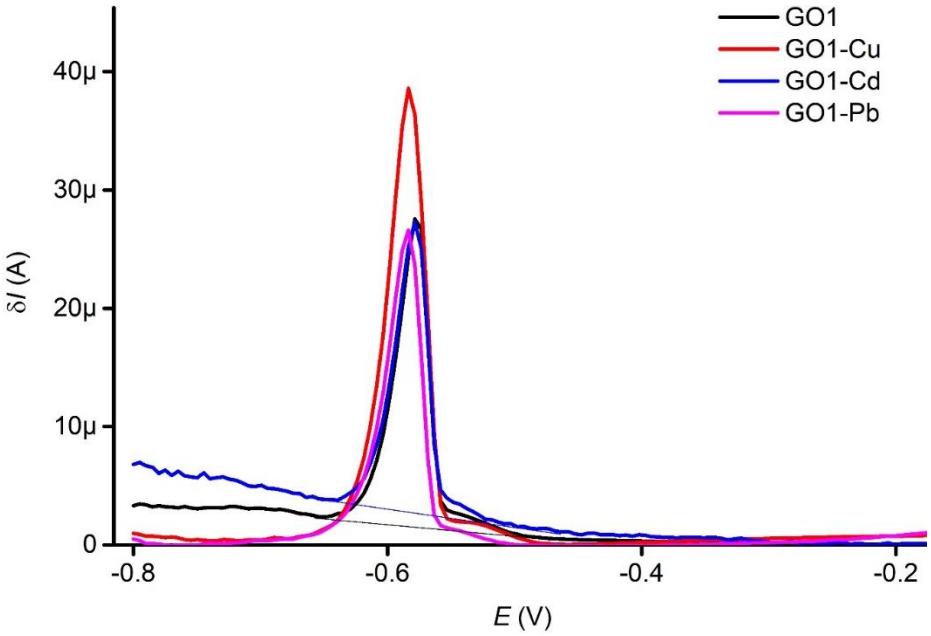

Figure 1: Illustrative ASSWV peaks acquired with GO1 (black), GO1-Cu (red), GO1-Cd (blue) and GO1-Pb (cyan) in 0.1M KCl acidified to pH=2 containing 1 ppm of Pb^{2+}. Flow speed 1.8 mL min^{-1}, resting time before the deposition 3 min, deposition time 20 s, deposition potential -1 V. Thick lines at GO1 and GO1-Cd data indicate baseline of the peaks.

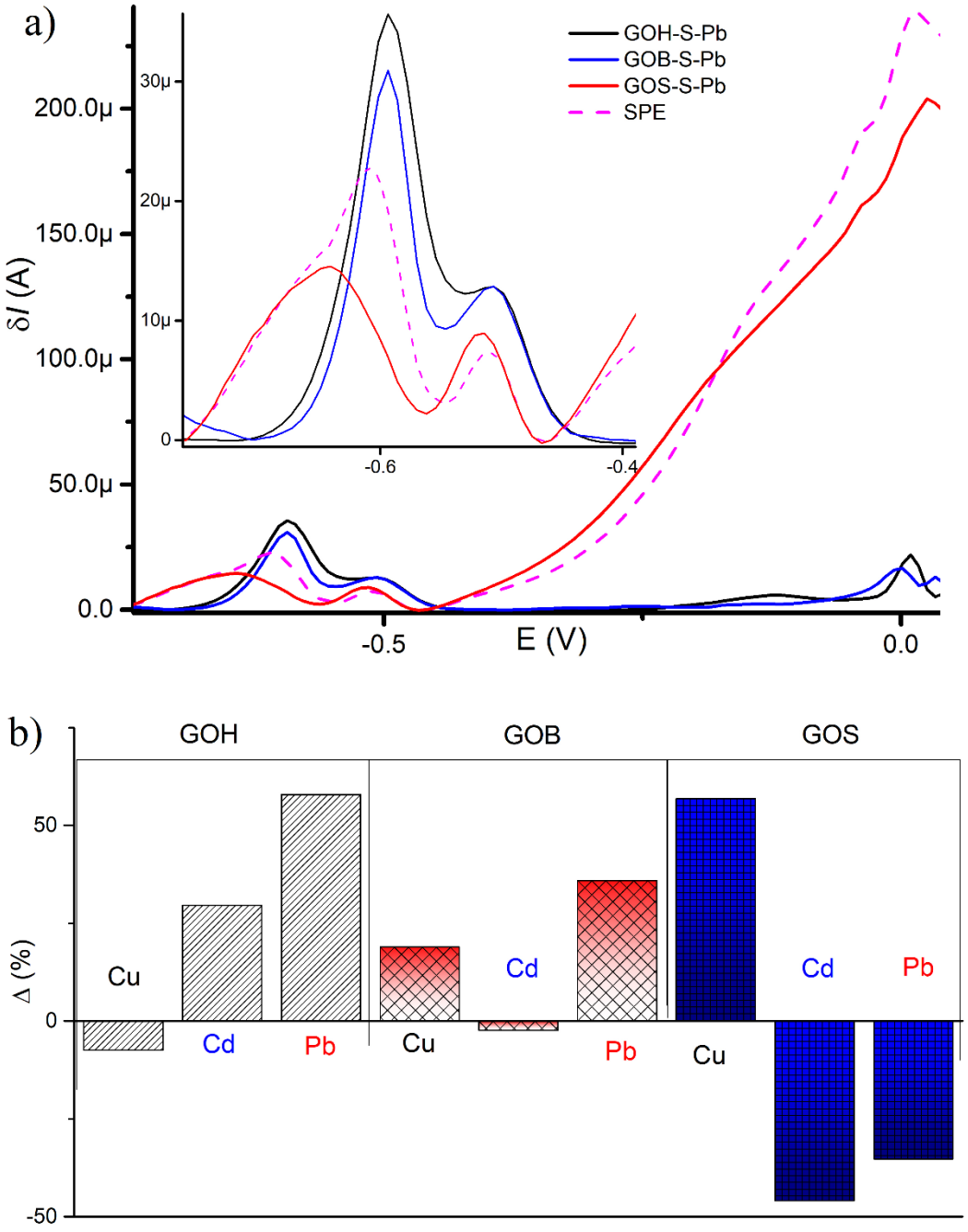

Figure 2: **a)** anodic stripping square wave voltammograms of GOx-S-Pb (black for GOH, blue for GOB and red for GOS) and unmodified SPE electrode (dashed magenta curve). **b)** relative change of ASSWV peak height (Δ, in %) acquired with GOx-S-m compared to the ASSWV peak achieved with unmodified SPE. All data acquired in a flow cell with 0.1 M KCl electrolyte acidified to pH = 2 and containing 1 ppm Pb^{2+} circulating in the system with the speed of 0.33 mL min^{-1}.

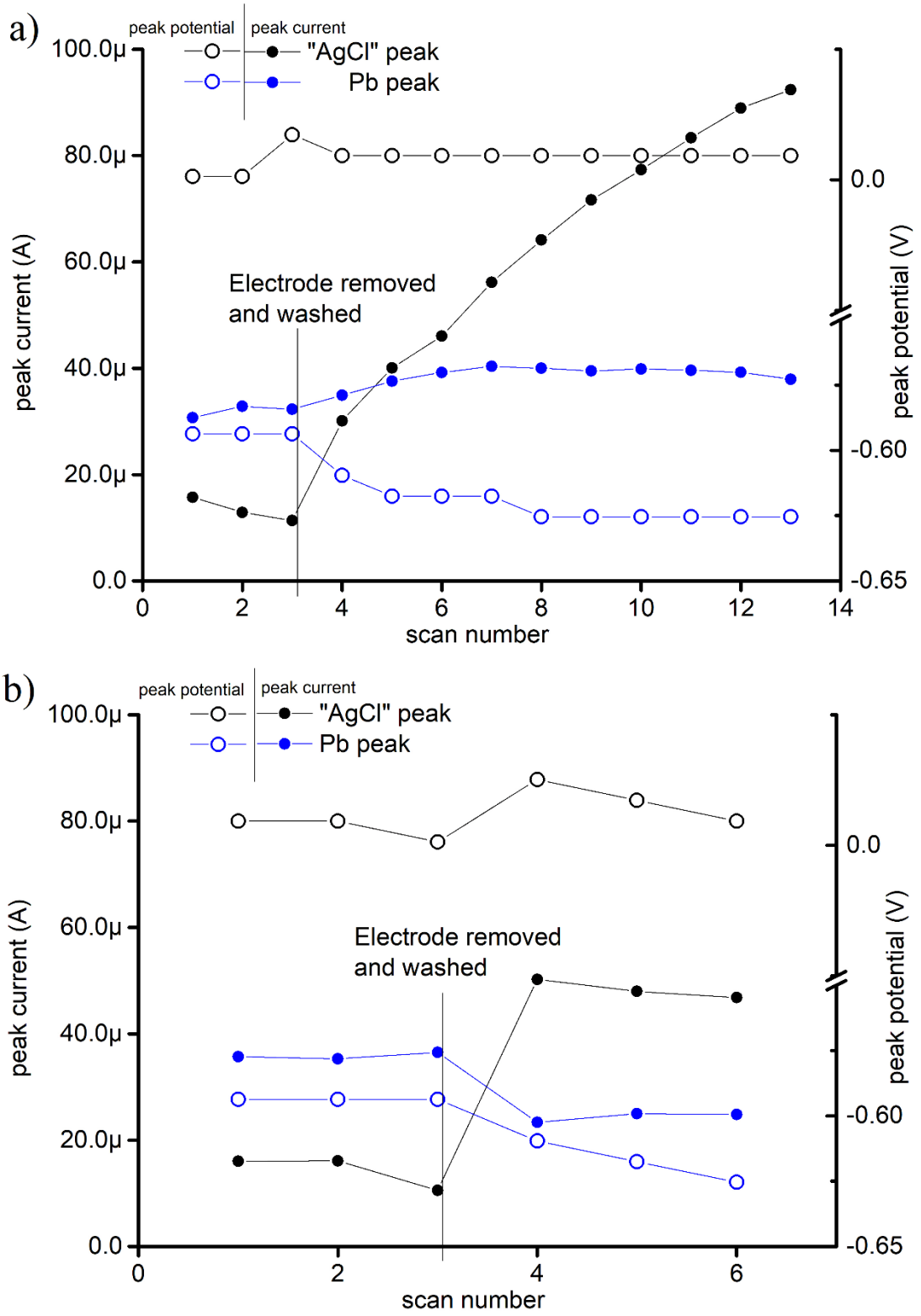

Figure 3: ASSWV peak heights (filled points, black – "AgCl" peak, blue – Pb peak) and potentials (hollowed points, black – "AgCl" peak, blue – Pb peak) achieved with GOB-S-Pb **(a)** and GOH-S-m **(b)** after repeated ASSWV measurements (horizontal axis, scan number). After three initial measurements the electrode was replaced and rinsed with DW, which is marked in the plot. All data acquired in a flow cell with 0.1 M KCl electrolyte acidified to pH = 2 and containing 1 ppm Pb^{2+} circulating in the system with the speed of 0.33 mL min^{-1}.

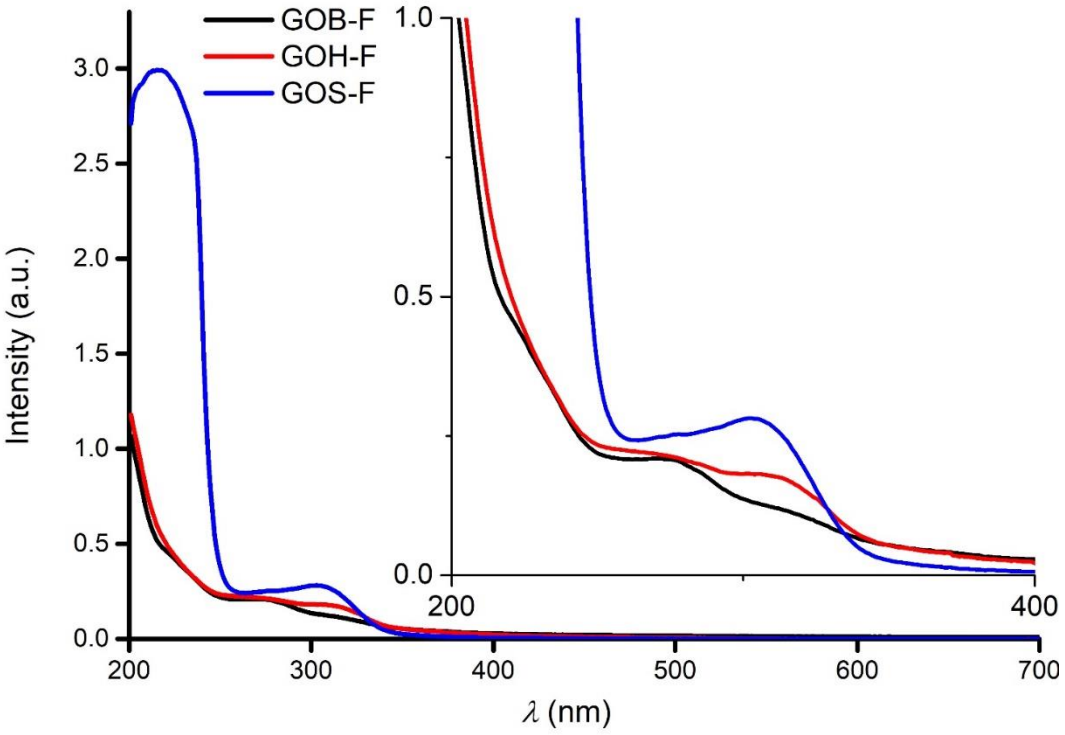

Figure 4: UV-vis spectra of GOB-F (black), GOH-F (red) and GOS-F (blue) aqueous dispersions. Insight – enlarge of the spectra.

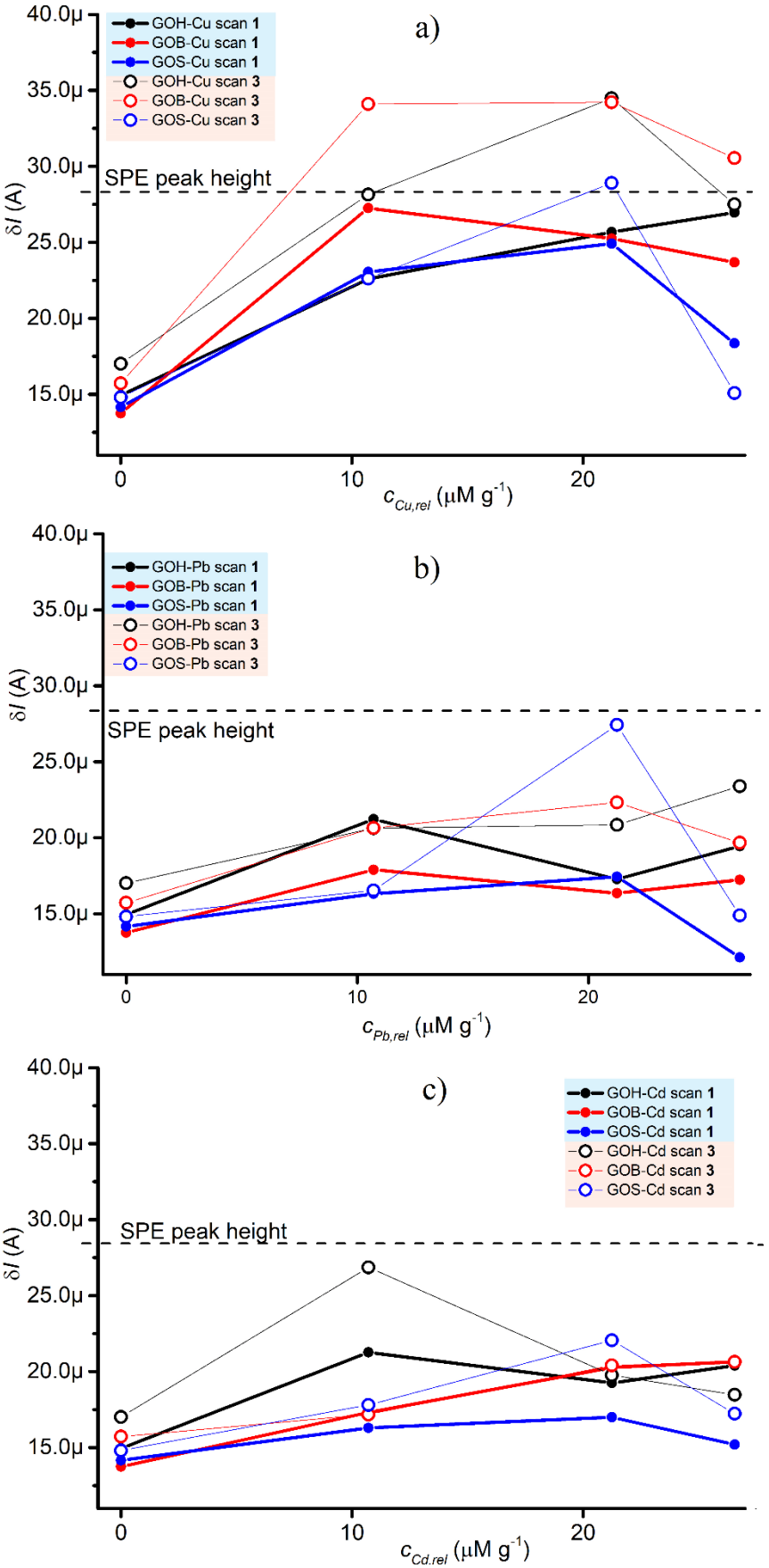

Figure 5: Absolute values of ASSWV peak heights achieved with GOx-F-Pb (**a)**), GOx-F-Cd (**b)**) and GOx-F-Cd (**c)**) sensors prepared with different relative concentration of "imprinting" metal cations (horizontal axes). Thick lines and filled dots represent values acquired from 1st ASSWV scans while thin lines and empty dots represent values acquired from consecutive 3rd scans. In all graphs average response of the unmodified SPE electrode is indicated by the dashed black line.

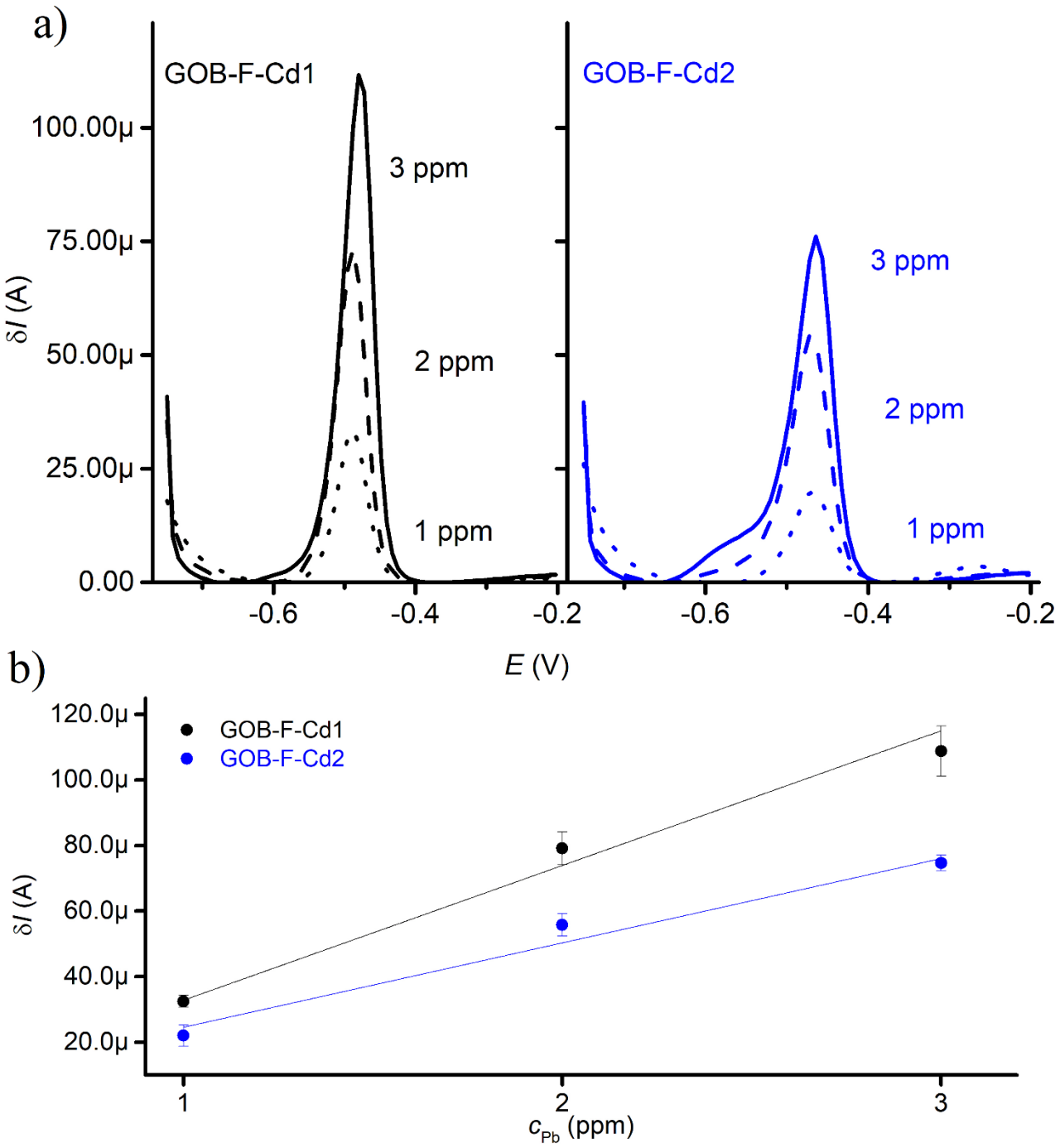

Figure 6: **a)** illustrative ASSWV voltammograms achieved with GOB-F-Cd1 (left, black curves) and GOB-F-Cd2 (right, blue curves) from 50 µL of 0.1 KCl acidified to pH=2 containing 1 (dotted), 2 (dashed) and 3 (solid) ppm of Pb^{2+}. **b)** calibration curves of GOB-F-Cd1 (black) and GOB-F-Cd2 (blue) acquired by evaluation of the data illustrated in panel a).

IMPRINTING OF DIFFERENT TYPES OF GRAPHENE OXIDE WITH METAL CATIONS

ELECTRONIC SUPPLEMENTARY INFORMATION

Authors: Piotr Zabierowski[a,b], Josef Osička[c], Josef Šťastný[a], Jaroslav Filip[a*]

[a] Department of Environmental Protection Engineering, Tomas Bata University in Zlin, Faculty of Technology, Nad Ovcirnou 3685, Zlin 760 01, Czechia

[b] CNR – Istituto per i Processi Chimico-Fisici, Sezione di Bari, via E. Orabona, 4, 70126, Bari, Italy

[c] Centre of Polymer Systems, Tomas Bata University in Zlin, Trida Tomase Bati 5678, Zlin 760 01, Czechia

* corresponding author: J. Filip, e-mail jfilip@utb.cz

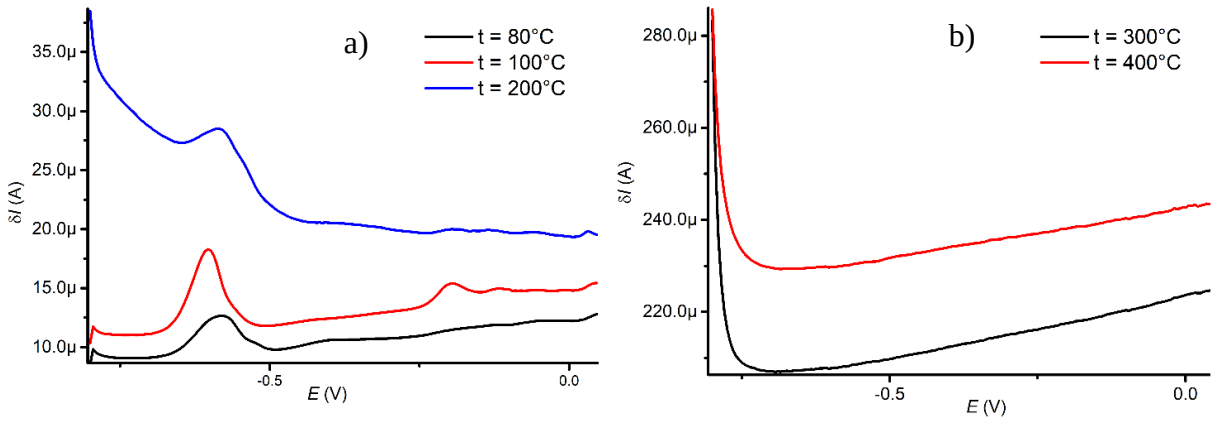

Figure S1. ASSWV of GO1-Pb treated at different temperatures (**a)** 80 – 200 °C, **b)** 300 and 400°C), indicated in the graph.

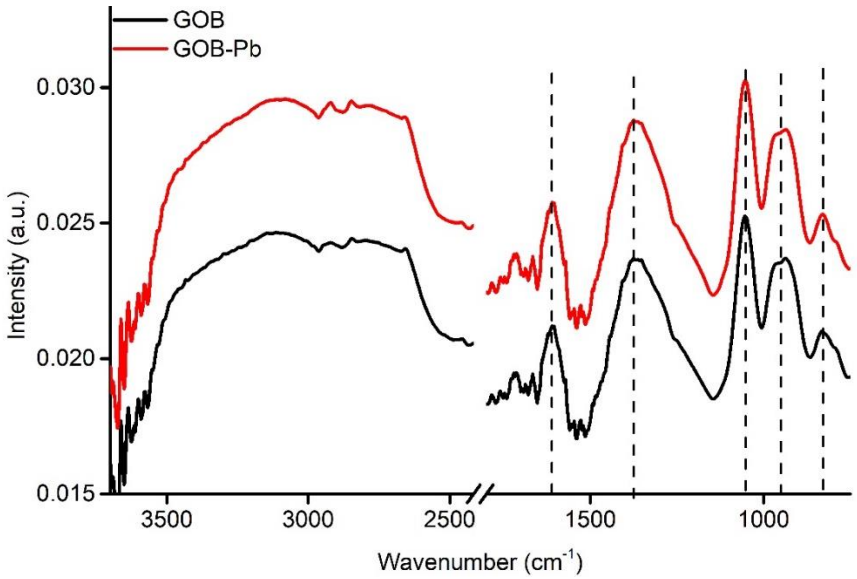

Figure S2. FTIR spectra of GO1 (GOB, black curve) and GO1-Pb (GOB-Pb, red curve) materials deposited on alumina foil and treated at 100°C for 15 min. Dashed vertical lines mark the major absorption peaks.

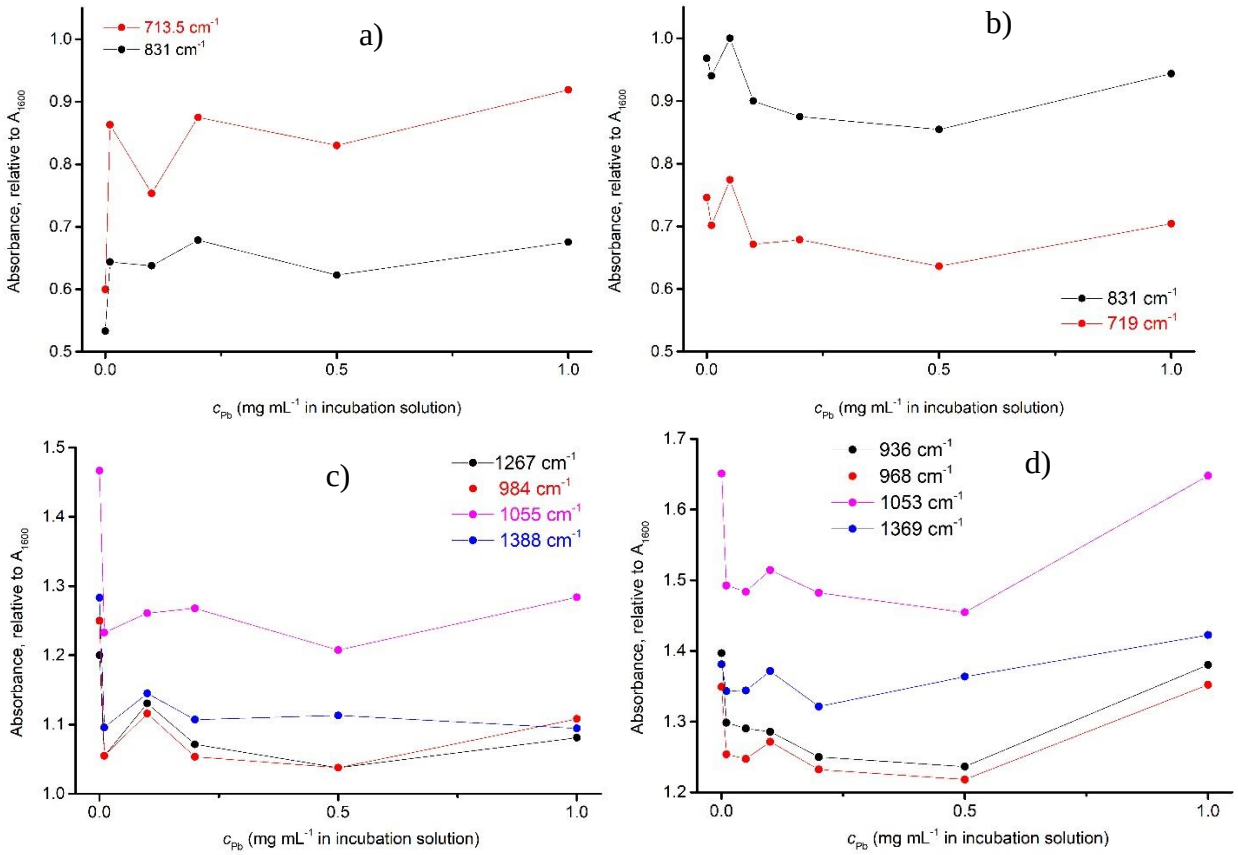

Figure S3. FTIR absorbance intensities of bands at 831 (black in **a)** and **b)**), 713.5 and 719 (red, in **a)** and **b)**, respectively), 1053-1055 (cyan in **c)** and **d)**), 1388 and 1369 cm^{-1} (blue in **c)** and **d)**, respectively), 984 and 968 cm^{-1} (red in **c)** and **d)**, respectively) and 1267 and 936 cm^{-1} (black in **c)** and **d)**, respectively) plotted towards concentration of Pb^{2+} in the incubation solution. Peak heights are related to the height of the peak at 1600 cm^{-1} for all samples. **a)** and **c)** – data for GO1-Pb prepared from GO**H**, **b)** and **d)** – data for GO1-Pb prepared from GO**B**.

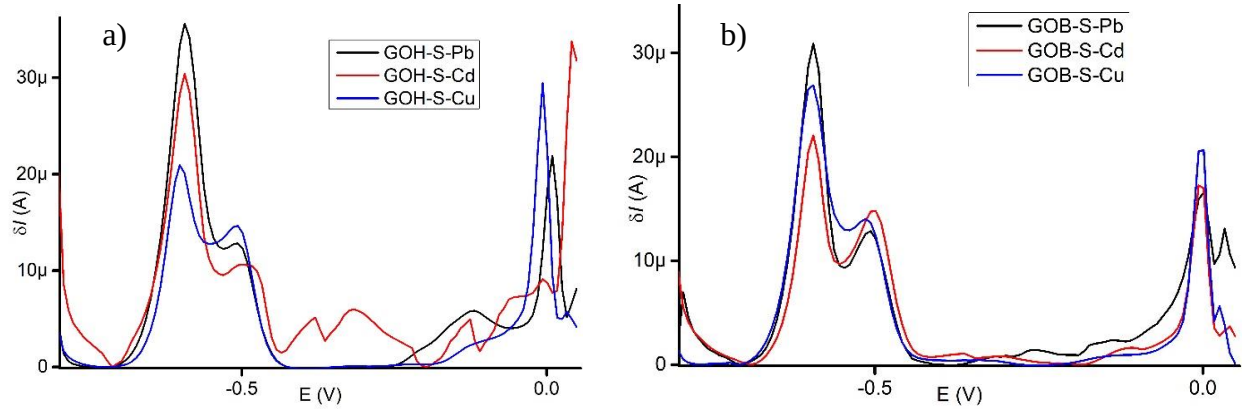

Figure S4. ASSWV voltammograms of GOH-S-m (**a)**) and GOB-S-m (**b)**). Deposition potential -1.0 V, deposition time 60 s, modulation amplitude 0.02 V and frequency 25 Hz.1 ppm of Pb^{2+} in 0.1 M potassium chloride acidified with nitric acid. Flow speed 0.33 mL/min.

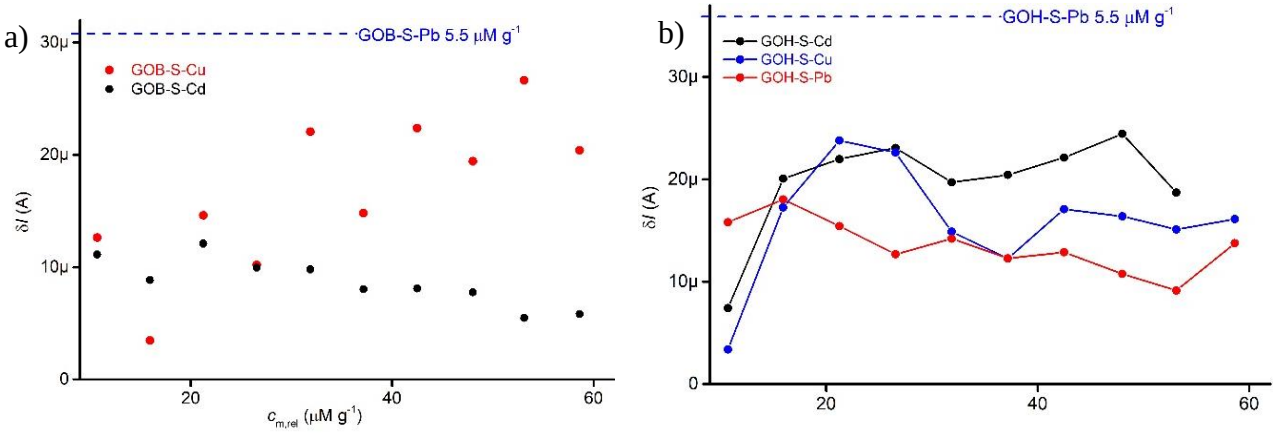

Figure S5. ASSWV peak heights of GO**B**-S-m (**a)**) and GO**H**-S-m (**b)**) prepared with different concentration of the respective metal cations in the precursor GOx-S-m solution. This is expressed as the $c_{m,rel}$ in μM of metal cation per 1 g of GOx-S. Blue dashed lines – markers of the achieved peak height when 5.5 μM g^{-1} of Pb^{2+} in GOx-S-Pb was used. Deposition potential -1.0 V, deposition time 60 s, modulation amplitude 0.02 V and frequency 25 Hz.1 ppm of Pb^{2+} in 0.1 M potassium chloride acidified with nitric acid. Flow speed 0.33 mL/min.

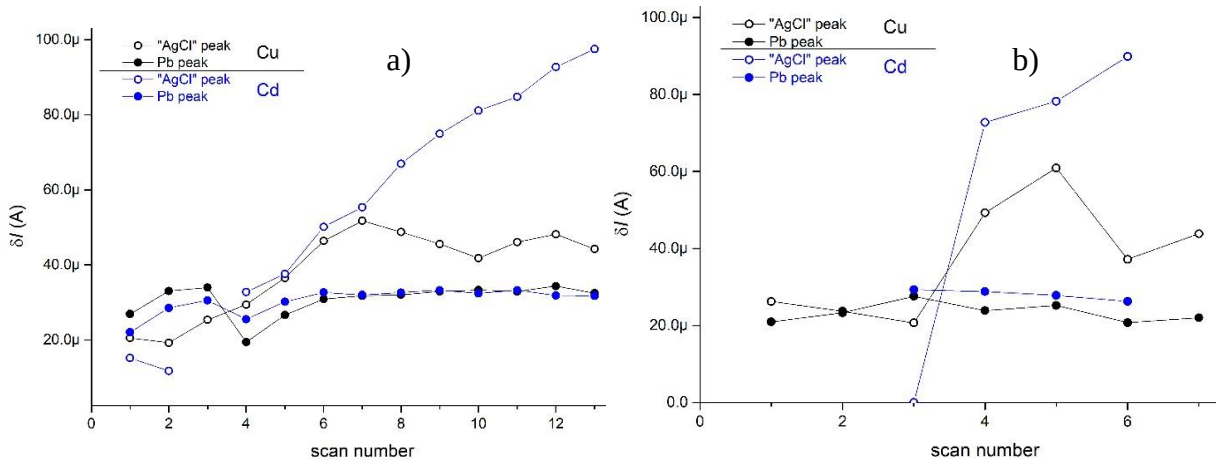

Figure S6. The ASSWV peak current of lead oxidation acquired with GOB-S-Cu (black) and GOB-S-Cd (blue) (**a)**) and GOS-S-Cu (black) and GOS-S-Cd (blue) (**b)**). Deposition potential -1.0 V, deposition time 60 s, modulation amplitude 0.02 V and frequency 25 Hz.1 ppm of Pb^{2+} in 0.1 M potassium chloride acidified with nitric acid. Flow speed 0.33 mL/min.

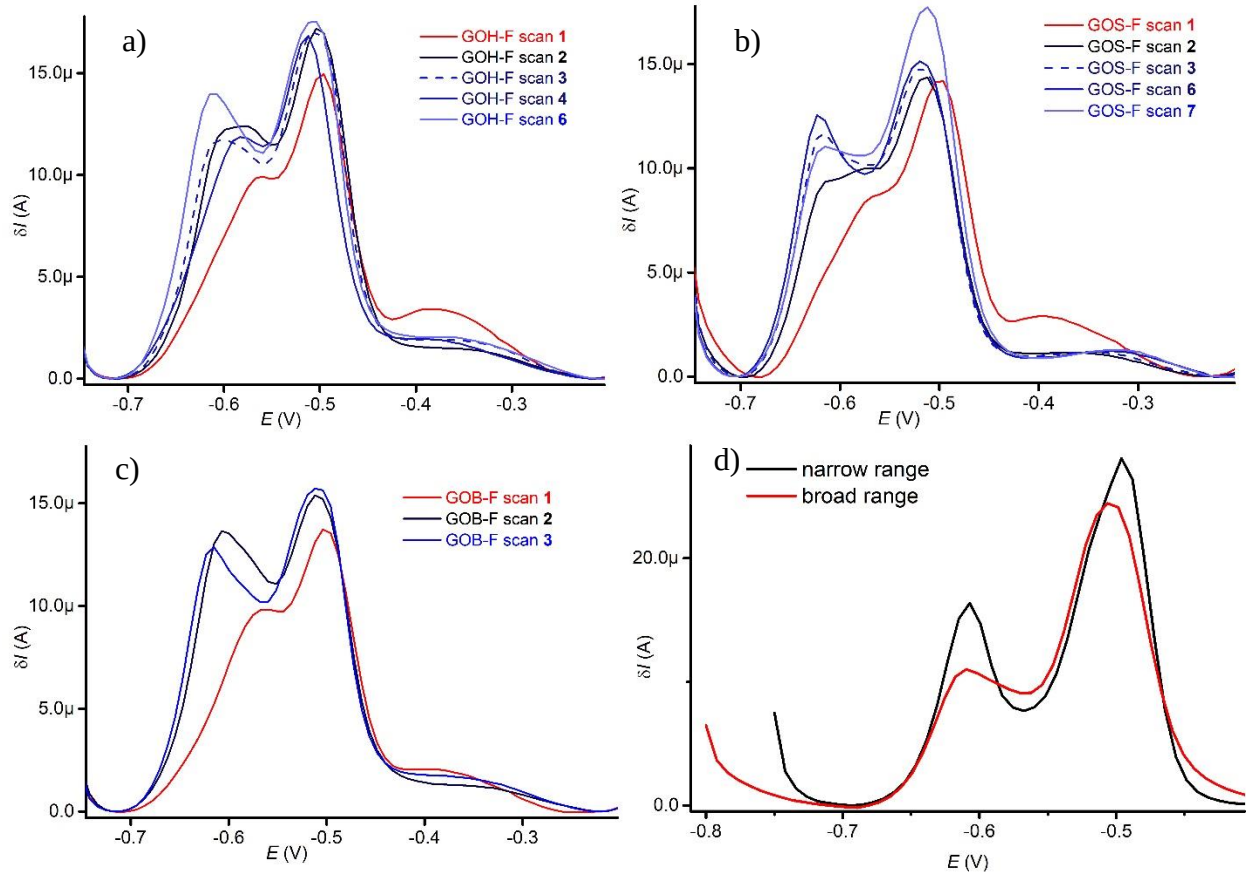

Figure S7. The ASSWV voltamograms measured consequently with GO**H**-F (**a)**), GO**S**-F (**b)**), GO**B**-F (**c)**) and pristine SPEs (**d)**). Scan numbers are indicated in the respective graphs. Deposition potential -1.0 V, deposition time 60 s, modulation amplitude 0.02 V and frequency 25 Hz. Room temperature, lead concentration 1 ppm in 0.1 M potassium chloride, pH=1.5 circulated in the flow cell with velocity of 0.33 mL/min. All curves acquired in potential range -0.75 → -0.2 V (against the SPEs´ reference electrodes), except for red curve in **d)** where the potential range was -0.8 → 0.2 V.